2014 IEEE International Conference on Robotics & Automation (ICRA)
Hong Kong Convention and Exhibition Center
May 31 - June 7, 2014. Hong Kong, China

Optimal Control Approach for Pneumatic Artificial Muscle with using Pressure-Force Conversion Model

Tatsuya Teramae[1], Tomoyuki Noda[1] and Jun Morimoto[1]

***Abstract*— In this paper, we propose an optimal control framework for pneumatic actuators. In particular, we consider using Pneumatic Artificial Muscle (PAM) as a part of Pneumatic-Electric (PE) hybrid actuation system. An optimal control framework can be useful for PE hybrid system to properly distribute desired torque outputs to the actuators that have different characteristics. In the optimal control framework, the standard choice to represent control cost is squared force or torque outputs. However, since the control input for PAM is pressure rather than the force or the torque, we should explicitly consider the pressure of PAM as the control cost in an objective function of the optimal control method. We show that we are able to use pressure input as the control cost for PAM by explicitly considering the model which represents a relationship between the pressure input and the force output of PAM. We demonstrate that one-DOF robot with the PE hybrid actuation system can generate pressure-optimized ball throwing movements by using the optimal control method.**

I. INTRODUCTION

Development of an exoskeleton robot to assist human movement is becoming a popular and important research topic. Especially, in the exoskeleton robot design, selection of actuators is an crucial issue since the actuators need to be light but need to generate large enough torque in order to assist both a user and the robot weights. To satisfy the above requirements, one possible approach would be using a Pneumatic Air Muscle (PAM) which has high force-to-weight ratio.

PAMs have been used to construct light weight legged robots and assistive devices [2], [14], [13], [12]. PAMs are mechanically compliant, and this property is also suitable for the exoskeleton design in terms of safety. On the other hand, using PAMs to precisely control endeffector positions or joint angles is not easy due to the complexity of air dynamics. To cope with this difficulty, in prevoius studies in our and other groups, simultaneous usage of electric motors and PAMs as a hybrid actuation system has been proposed [9], [2], [3], [4], [5]. The basic strategy of this hybrid control approach is using light-weight electric motors to generate precise motion and using light-weight PAMs to generate large forces. Then, to distribute desired torque to two kinds of actuators, we can use optimal control framework as we did in our prevoius studies [1], [5]. However, in this optimal control approache, we considered torque outputs of PAMs and electric motors as the control inputs to the robot. Therefore, to control PAMs, we additionally needed to derive pressure inputs to generate the optimized torque outputs for PAMs. On the other hand, since torque which can be generated by PAMs depends on contraction rate and pressure, PAMs may not be able to generate desired torque derived by the opmital control framework which do not explicitly consider the contraction rate.

In this study, we newly propose a method to optimize pressue input to control a robot, which has the hybrid actuation system composed of a PAM and an electric motor, by explictly considering a pressure-torque conversion model for the PAM. By taking the pressure input of the PAM into account, the torque output derived by the optimal control framework becomes a feasible solution. We apply our proposed approach to control a one degrees-of-freedom (DOF) arm robot system.

In the following section, we introduce pressure-torque conversion model for the PAM, and explain how we optimize the pressure of the PAM and toruqe of the electric motor by using the iterative LQG method [7]. Finally, we show control performances of our proposed method when we apply the method to control the one-DOF robot to throw a ball into a hoop.

II. MODELING OF PE HYBRID ONE-DOF SYSTEM

This section introduces the model of PAM and one-DoF system.

Figure 1 shows developed exoskeleton robot XoR and one-DoF system with PE hybrid actuator. One-DoF system has one motor and two PAM, but in this study PAM uses one PAM only. Because a knee joint of XoR has not an antagonistic muscle and we can verify that our approach can be applied to knee joint of XoR with limited actuation component.

A. pressure-force model

PAM contracts by injecting the air flow to PAM from air tank and force of PAM F is provided by contraction. This force is transferred to a joint through a wire and is converted to joint torque of PAM τ_p through a p ulley. τ_p is

$$\tau_p = rF, \tag{1}$$

where r is a radius of the pulley. Figure 2 shows fitting results between force and contraction rate in each constant pressure. When the pressure of PAM is constant, force and contraction of PAM can be fit by quadratic equation shown in figure 2. Moreover, a relation between the pressure and the force of PAM has linearity when the contraction rate is constant (Vertical line (a) in figure 2). Therefore, if contraction rate set constant value, conversion model from pressure to force

[1]Department of Brain Robot Interface, ATR Computational Neuroscience Laboratories, Kyoto, Japan

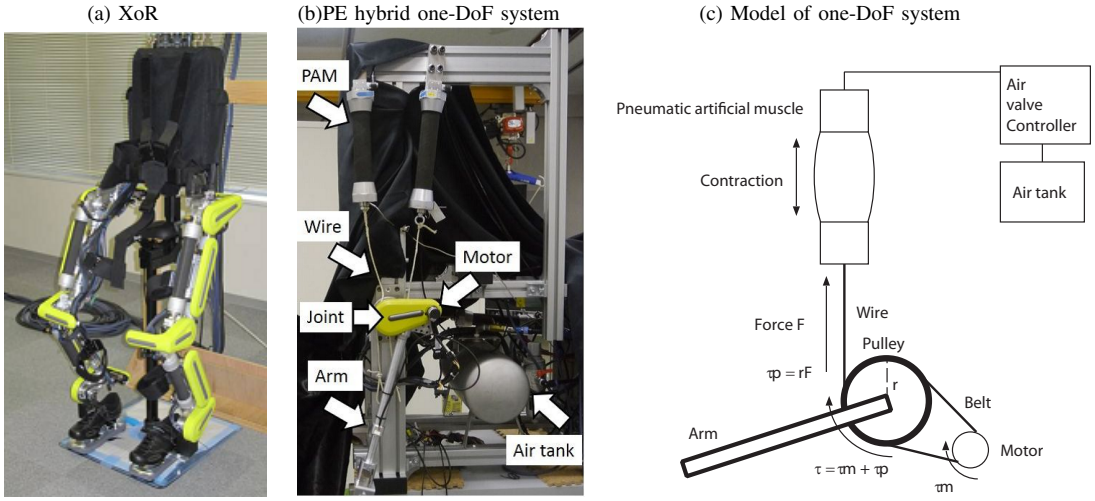

Fig. 1. Exoskeleton robot for lower human body: XoR has 6 joint with PE hybrid actuation system. One Degree of Freedom(DoF) system: This system is same as XoR one joint and equips pneumatic artificial muscles and electric motor. One-DoF system condition: Mass is 1.7 kg. Arm length and center of mass length are both 0.4 m. Electric motor is maxon EC 4 pole 399401 200 W. PAM is provided by FESTO. Air valve is provided by NORGREN

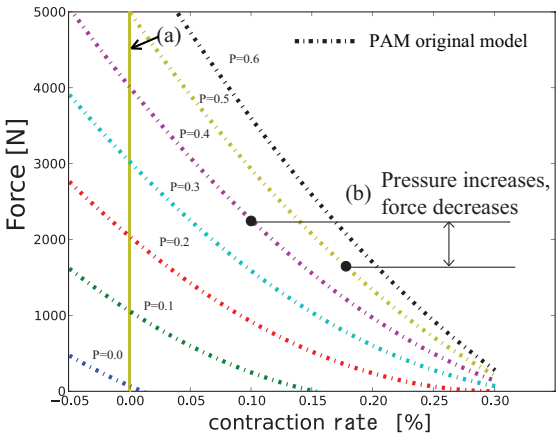

Fig. 2. Fitting result of contraction rate and force of PAM in each constant pressure. Horizontal axis is contraction rate. Vertical axis is force. Those caves are fitting plot by virtual data of data sheet provided by FESTO.

can be written by a linear equation. Assuming all states are in equilibrium states, force of PAM F is written by

$$F = \frac{(f_u - f_l)P + P_u f_l - P_l f_u}{P_u - P_l} \tag{2}$$

where P is the inner pressure of PAM. P_u and P_l are constant pressure 0.8 MPa and 0.7 MPa [14]. f_u is a quadratic force model when pressure is set 0.8 MPa and f_l is a quadratic force model when pressure is set 0.7 MPa.

$$f_u = a_u\alpha^2 + b_u\alpha + c_u, \tag{3}$$

$$f_l = a_l\alpha^2 + b_l\alpha + c_l. \tag{4}$$

Each parameter a_u, b_u, c_u, a_l, b_l and c_l are shown in TABLE I. α is contraction rate calculated by joint angle as follows

$$\alpha = \frac{r(\theta - \theta_{min})}{l_{pam}}. \tag{5}$$

TABLE I

COEFFICIENT IN QUADRATIC FORCE MODEL

a_l, b_l, c_l	22142, -13431, 2031
a_u, b_u, c_u	5426, -32110, 9839

θ, θ_{min} and l_{pam} are joint angle, minimal joint angle and natural length of PAM.

$(f_u - f_l)$ in (2) are the monotonic decrease function in usable range of pressure-force model. This pressure-force model 2 shows that, even if the pressure of PAM increases, the force of PAM decreases when contraction increases (Figure 2 (b)). Therefore, the directly optimization of pressure is an important issue for PAM energy resource.

B. Implementation of pressure-force model to one-DoF system

We introduce the model of one-DoF system implementing pressure-force model. State equation is

$$\dot{\boldsymbol{x}} = \boldsymbol{f}(\boldsymbol{x}, \boldsymbol{u}) = \boldsymbol{A}_s\boldsymbol{x} + \boldsymbol{B}_s\boldsymbol{u} + \boldsymbol{H}_e. \tag{6}$$

State variable $\boldsymbol{x}$ includes joint angle θ, angular velocity $\dot{\theta}$ and measured inner pressure of PAM P.

$$\boldsymbol{x} = \begin{bmatrix} \theta & \dot{\theta} & P \end{bmatrix}^T \tag{7}$$

Input $\boldsymbol{u}$ is set reference inner pressure P_{ref} and motor torque τ_m.

$$\boldsymbol{u} = \begin{bmatrix} P_{ref} & \tau_m \end{bmatrix}^T$$

The dynamics between the reference pressure P_{ref} and measured inner pressure P has nonlinear characteristics according to air dynamics, but dynamics is approximated by the first oder lag system in this study, because the inner pressure P is controlled by the air valve controller as a regulator. Therefore, dynamics between P_{ref} and P is

$$P = \frac{1}{1 + t_c s}P_{ref} \tag{8}$$

TABLE II

MODEL CONDITIONS

Mass(m)	1.7[kg]
Length(l)	0.4[m]
Joint friction(μ)	0.169[Ns/m]
Inertia(I)	0.272[kg/s^2]
Sampling time(Δt)	0.004[s]

where t_c is time constant and set as follows

$$t_c = \begin{cases} 0.08 & (\dot{\tau_p} > 0) \\ 0.4 & (otherwise) \end{cases} \tag{9}$$

If $\dot{\tau_p}$ is positive, the air is injected into PAM and t_c is decided from step response when pressure is changed from 0 MPa to 0.8 MPa. On the other hand, if the air is ejected from PAM, t_c is decided by step response from 0.8 MPa to 0 MPa. This time constant t_c is a PAM response limitation, because the time constant when $\dot{\tau_p}$ is negative is very slow compared with the motor response. The motor dynamic is no time lag in this study, because the motor has enough following performance compared with PAM.

$\boldsymbol{A}_s$ and $\boldsymbol{B}_s$ include first order lag system and linear term of pressure-force model (2).

$$\boldsymbol{A}_s = \begin{bmatrix} 0 & 1 & 0 \\ 0 & -I^{-1}\mu & I^{-1}(1 - r\frac{fu-fl}{Pu-Pl}(1 - e^{-\frac{\Delta t}{t_c}})) \\ 0 & 0 & -\frac{1-e^{-\frac{\Delta t}{t_c}}}{\Delta t} \end{bmatrix},$$

$$\boldsymbol{B}_s = \begin{bmatrix} 0 & 0 \\ I^{-1}(r\frac{f_u-f_l}{P_u-P_l}(1 - e^{-\frac{\Delta t}{t_c}})) & I^{-1} \\ \frac{1-e^{-\frac{\Delta t}{t_c}}}{\Delta t} & 0 \end{bmatrix}$$

Moreover, $\boldsymbol{H}_e$ includes the non-linear terms as a extra torques. The extra torques are gravity term and nonlinear term of pressure-force model (2).

$$\boldsymbol{H}_e = \begin{bmatrix} 0 \\ I^{-1}(mgl\sin\theta + r\frac{P_u f_l - P_l f_u}{P_u - P_l}) \\ 0 \end{bmatrix}$$

Each variables of $\boldsymbol{A}_s$, $\boldsymbol{B}_s$ and $\boldsymbol{H}_e$ are shown in TABLE II. Joint friction μ is kinetic friction, and joint friction and inertia are estimated based on the calibration data when arm fall down from 180 deg.

III. OPTIMIZATION FOR PE HYBRID ACTUATOR BY ITERATIVE LQG METHOD

This section introduces the iterative LQG method as the optimal control for PE hybrid actuator.

The optimization problem for one-DoF system as (6) is to find control policy to minimize the objective function. If the target dynamic is a linear model and objective function is defined by the quadratic equation using state variables and control inputs, the optimization problem can be solved by using Linear Quadratic Regulator (LQR). In this case, the dynamics of PE hybrid one-DoF system is nonlinear. Then, several algorithms that find a locally optimal policy for nonlinear function had been proposed such as Differential Dynamic Programming (DDP) [6] and iterative LQG method [7]. In this study, we used an iterative LQG method as optimal control for PE hybrid actuator.

The iterative LQG method can solve an optimization problem for nonlinear model, because the iterative LQG method solves iteratively linearized quadratic Gaussian problem around the reference trajectory in each sampling time.

A new control input $\boldsymbol{u}_{k+1}$ is calculated by

$$\boldsymbol{u}_{k+1} = \boldsymbol{u}_k + \dot{\boldsymbol{u}}_k \Delta t \tag{10}$$

where k is sampling number. Since the dynamic is linearized and the objective function is approximated to quadratic form at around the reference trajectory in each step k, the LQG problem is solved using Riccati-like equations [7]. Control law $\dot{\boldsymbol{u}}_k$ is

$$\dot{\boldsymbol{u}}_k = \boldsymbol{l}_k + \boldsymbol{L}_k \Delta t. \tag{11}$$

$\boldsymbol{l}$ and $\boldsymbol{L}$ are

$$\boldsymbol{l}_k = -\boldsymbol{H}_k^{-1}\boldsymbol{g}_k, \boldsymbol{L}_k = -\boldsymbol{H}_k^{-1}\boldsymbol{G}_k. \tag{12}$$

$\boldsymbol{l}$ is open loop term and $\boldsymbol{L}$ is feedback term.

$\boldsymbol{H}, \boldsymbol{G}, \boldsymbol{g}$ are

$$\boldsymbol{H} = \boldsymbol{R}_k + \boldsymbol{B}_k^T \boldsymbol{S}_{k+1} \boldsymbol{B}_k, \tag{13}$$

$$\boldsymbol{G} = \boldsymbol{P}_k + \boldsymbol{B}_k^T \boldsymbol{S}_{k+1} \boldsymbol{A}_k, \tag{14}$$

$$\boldsymbol{g} = \boldsymbol{r}_k + \boldsymbol{B}_k^T \boldsymbol{S}_{k+1}, \tag{15}$$

where, $\boldsymbol{A}_k, \boldsymbol{B}_k$ are defined as follows

$$\boldsymbol{A}_k = \boldsymbol{I}_n + \Delta t \frac{\partial \boldsymbol{f}}{\partial \boldsymbol{x}}, \boldsymbol{B}_k = \Delta t \frac{\partial \boldsymbol{f}}{\partial \boldsymbol{u}}.$$

$\boldsymbol{I}_n$ is n order unit matrix, $\boldsymbol{f}$ is a state equation (6), J is objective function when k, $\boldsymbol{x}$ is a state variable, $\boldsymbol{u}$ is input, and $\boldsymbol{r}_k, \boldsymbol{R}_k$ are

$$\boldsymbol{r}_k = \Delta t \frac{\partial J_k}{\partial \boldsymbol{u}}, \boldsymbol{R}_k = \Delta t \frac{\partial^2 J_k}{\partial \boldsymbol{u} \partial \boldsymbol{u}}.$$

$\boldsymbol{P}_k$ is

$$\boldsymbol{P}_k = \Delta t \frac{\partial^2 J_k}{\partial \boldsymbol{u} \partial \boldsymbol{x}}.$$

$\boldsymbol{S}_k, \boldsymbol{s}_k$ are represented as

$$\boldsymbol{S}_k = \boldsymbol{Q}_k + \boldsymbol{A}_k^T \boldsymbol{S}_{k+1} \boldsymbol{A}_k - \boldsymbol{G}^T \boldsymbol{H}^{-1} \boldsymbol{G}, \tag{16}$$

$$\boldsymbol{s}_k = \boldsymbol{q}_k + \boldsymbol{A}_k^T \boldsymbol{S}_{k+1} - \boldsymbol{G}^T \boldsymbol{H}^{-1} \boldsymbol{g}, \tag{17}$$

where $\boldsymbol{q}_k, \boldsymbol{Q}_k$ are

$$\boldsymbol{q}_k = \Delta t \frac{\partial J}{\partial \boldsymbol{x}}, \boldsymbol{Q}_k = \Delta t \frac{\partial^2 J}{\partial \boldsymbol{x} \partial \boldsymbol{x}}.$$

IV. VERIFICATION SETUP

In this section, we introduce a task to verify the performance of our approach and the definition of the objective function to realize the task.

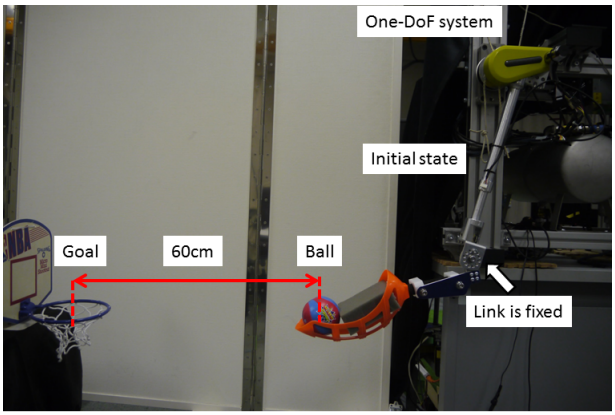

Fig. 3. Experimental equipment. Experimental task is that ball is thrown in the goal. Distance between initial position of ball and goal is 600 mm. Link between basket and arm of one-DoF is fixed.

A. Task setup

Figure 3 shows the setup of a verification task. This task is that the ball is thrown by one-DoF system and shoot into the goal in the position distance 600 mm. To achieve this task needs high speed motion and accurate position and velocity control. Such a performance required also to driver safety the exoskeleton robot for human. A control performance of our approach and accuracy of the structured model can be verified by this task.

B. Objective function for PE hybrid actuator

The error between target and measured value E_a and E_v are defined as follow

$$E_a(t) = \theta(t) - \theta_{ref}(t), \tag{18}$$

$$E_v(t) = \dot{\theta}(t) - \dot{\theta}_{ref}(t), \tag{19}$$

where t is time, θ_{ref} is target angle $\dot{\theta}_{ref}$ is target angular velocity.

An input cost for minimization of torque was set as follow

$$u_{c\tau}(t) = w_{pn}\tau_p^2(t) + w_m\tau_m^2(t). \tag{20}$$

In previous study [5], the objective function in final state was set as

$$J_\tau(T_f) = w_{pf}E_a^2(T_f) + w_{vf}E_v^2(T_f) + u_{c\tau}(T_f), \tag{21}$$

the objective function in given time was set as

$$J_\tau(T_{th}) = w_pE_a^2(T_{th}) + w_vE_v^2(T_{th}) + u_{c\tau}(T_{th}), \tag{22}$$

and running cost was set as

$$J_\tau(k) = u_{c\tau}(k). \tag{23}$$

T_{th} is given time and T_f is final time. w_p, w_v, w_{pf}, w_{vf}, w_{pn} and w_m are weight coefficient. The objective function minimizes summation of squared motor torque τ_m and squared PAM torque τ_p. This also minimizes the squared error between the joint angle and the target angle θ_{ref} and between the joint angular velocity and the target angular velocity $\dot{\theta}_{ref}$. We set target angles and velocities in giving time and final time, because an achievement to a necessary positive velocity and a necessary negative velocity in given timing and given angle is required for success in the ball throwing.

However, this function did not consider the pressure of PAM. An input cost for minimization of PAM pressure was set as follow

$$u_{cP}(t) = w_{pn}P^2(t) + w_m\tau_m^2(t). \tag{24}$$

In this study, we use the pressure of PAM term as PAM input in the objective function instead of torque of PAM τ_p as follows

$$J_P(T_f) = w_{pf}E_a^2(T_f) + w_{vf}E_v^2(T_f) + u_{cP}(T_f), \tag{25}$$

objective function in given time was set as follows

$$J_P(T_{th}) = w_pE_a^2(T_{th}) + w_vE_v^2(T_{th}) + +u_{cP}(T_{th}), \tag{26}$$

and running cost was set

$$J_P(k) = u_{cP}(k) \tag{27}$$

This function can minimize the squared pressure of PAM that has nonlinear characteristics between torque and pressure.

V. Verification Results

A. Simulation

In simulation, we set two types objective functions (20) and (27) for optimal control. We decided target angle, velocity and timing T_{th} from trial data when human actually throw the ball using the one-DoF system.

Figure 4 shows the simulation results and conditions. Figure 4 (a) and (e) show that target angles in final state could be achieved. Error between target angular velocity and measured velocity in given time and final time were 0 and 0.3 rad/s in (a), 0 and 0. rad/s in (e). Therefore, we could get reference trajectory to achieve the target angle and velocity in each objective function.

Figure 4 (b) and (f) show that pressure optimized P was small expect around 1.5 s and pressure optimized τ_p was large pressure and has much changed. The summation of pressure in (b) and (f) are 25.15 and 53.57 MPa. The pressure was half compared with result of optimizing torque by optimizing pressure directly. Figure 4 (c) and (g) show that torque optimized P was large when angular velocity was positive and torque optimized τ was small in all time. Therefore, these results show that each objective function could be optimized by our approach.

Figure 4 (d) and (h) show that the motor torque in each figure were similar signal to achieve the target angle and velocity. The summation of motor torque in (d) and (h) are 606 and 655 Nm.

In torque distribution result of the motor and the PAM, the motor was used dominantly because this task needed a high speed to achieve target velocity and position in a final state and a system is light weight. On the other hand, the PAM with low response worked so as not to disturb the motor torque in results of torque optimization.

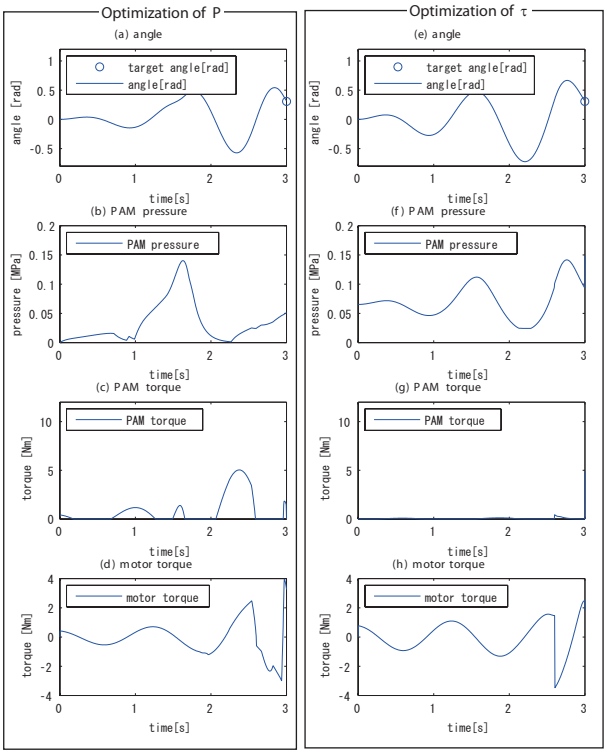

Fig. 4. Simulation results : (a) $\sim$ (d) show results that pressure of PAM was minimized (proposed method). (e) $\sim$ (h) show results that torque of PAM was minimized (conventional method). Vertical axis show angle in (a) and (e), pressure of PAM in (b) and (f), PAM torque in (c) and (g) and motor torque in (d) and (h). Simulation conditions : Experimental duration is 3[s]. Sampling frequency is 250[Hz]. Initial angle and velocity are 0. Target angle and velocity when 2.6 s are 0.35 rad and 4 rad/s. Target angle and velocity in final state are 0.31 rad and -2 rad/s. Objective function J_P weights are $w_p = 10^5$, $w_v = 10^4$, $w_{pf} = 10^5$, $w_{vf} = 10^5$, $w_{pn} = 100$, and $w_m = 1$. Objective function J_τ weights are $w_p = 10^5$, $w_v = 10^4$, $w_{pf} = 10^5$, $w_{vf} = 10^5$, $w_{pn} = 10$, and $w_m = 1$. Movable range is set as $-0.6 < \theta < 1.6$.

Compared with results of optimization of P and τ, the summation of pressure optimized P was smaller than the sum of pressure optimized τ, and the torque of PAM could be used to give aid to positive motor torque, but the results of optimizing τ show that the torque of PAM was almost 0 Nm so as not to disturb the motor and a lot of air had been used. Those results show that, even if the torque of PAM was minimized, the pressure of PAM was not necessarily minimized. Therefore, we could verify that the implement of pressure-force model to the optimal control was necessity to minimize the actual input of PAM and use effectively PAM torque.

B. Experiment

In the experiment, the reference pressures of PAM and torques of motor when optimized P and τ calculated by simulation is given to actual one-DoF system to verify the accuracy of our structured pressure-force model and control performance of optimal control.

Figure 5 shows that experimental flow. In the experiment, the input of PAM and motor has only been feed-forward

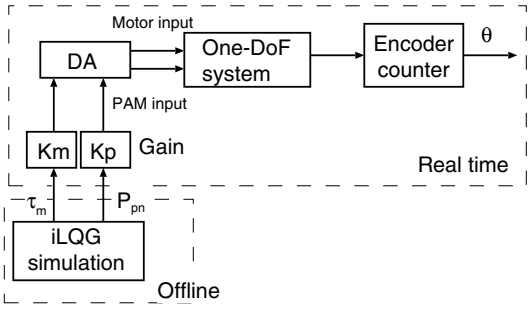

Fig. 5. Block diagram in experiment : The I/O signal communication between control PC and one-DoF system is realized by hard real-time system using Debian 7.0 with Xenomai 2.6.2 and RTnet. Xenomai is real-time kernel patch for Linux and RTnet is hard real-time networking for Xenomai.

input calculated by the iterative LQG method, and feed-forward input is tuned myself by proportion gain K_p and K_m because actual one-DoF system has model differential caused by wire laxity, joint static friction and joint inertia.

Figure 6 shows the experimental results and conditions. Figure 7 shows a snapshot of the experimental results. Figure 6 (a) and (b) show that measured angle followed a reference trajectory but there is an error between measured angle and reference one. Average of error in (a) is 0.05 rad and one in (b) is 0.07 rad. This error is caused by pressure-force model fitting error and kinetic model parameter (Inertia and kinetic friction) fitting error, because error between reference pressure and actual necessary pressure occurs by differing slightly angle and reference trajectory. However, figure 7 shows that flying distance of ball is almost same about 600 mm and ball throwing into the goal task was successful. Therefore, this result shows that accuracy of position and velocity control is enough to achieve ball throwing task. In result, we could verify that the PE hybrid actuation system can be controlled accurately by feed-forward inputs of PAM and motor calculated by our approach. Moreover, we could structure accuracy pressure-force model and one-DoF system model with PE hybrid actuator.

VI. CONCLUSIONS

We aimed to optimize directly the pressure of PAM using the iterative LQG method implemented pressure-force model of PAM. We verified that the reasonable pressure of PAM and torque of the motor could be calculated based on our approach implemented pressure-force model in simulation results, and the summation of PAM pressure was half compared with pressure when torque of PAM is optimized. Moreover, we verified the accuracy of structured models and control performance of one-DoF system using our approach by experiment that one-DoF system was controlled by only proportionally tuned feed-forward pressure input of PAM and torque inputs of motor calculated by the iterative LQG simulation. We could success the verification task that ball is thrown into the goal using one-DoF system. In conclusion, we could control accurately one-DoF system with PE hybrid actuator by our approach and could structure accuracy pressure-force model.

Fig. 7. Snapshot of experimental results : Ball throwing task. picture shows result that pressure was minimized.

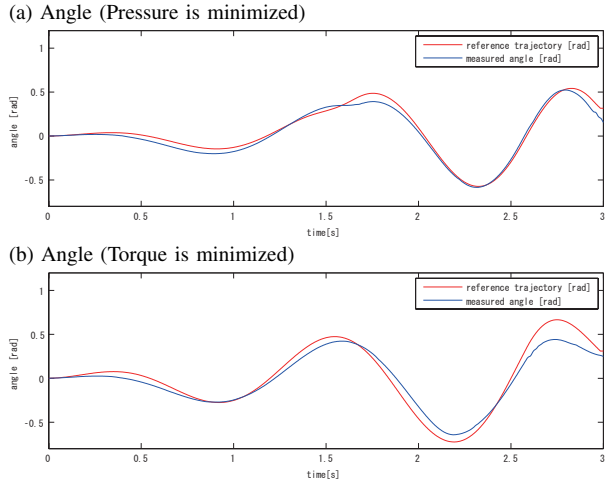

Fig. 6. Experimental results : (a) show results that pressure was minimized. (b) show results that pressure change was minimized. Horizontal axis is time. Vertical axis is angle. Red line is reference trajectory. Blue line is measured angle. Experimental conditions : Experimental duration is 10[s]. Sampling frequency is 250[Hz]. Proportion gain K_p and K_m in (a) are 1.3 and 1.4. K_p and K_m in (b) are 1.0 and 1.0.

ACKNOWLEDGMENT

This study is the result of SRPBS, MEXT. This work was also supported by the Strategic International Research Cooperative Program, Japan Science and Technology Agency (JST). This study is also result of MIC-SICP This research was supported by a contract with the Ministry of Internal Affairs and Communications entitled, 'Novel and innovative R& D making use of brain structures' The work of J. Morimoto was supported by the MEXT KAKENHI under Grant 23120004. This work was also supported by JSPS and MIZS under the Japan-Slovenia Research Cooperative Program. T. Noda was partially supported by KAKENHI Grant Number 24700203.

REFERENCES

[1] T. Matsubara, T. Noda, S. H. Hyon, J. Morimoto, "An Optimal Control Approach for Hybrid Actuator System," 2011 IEEE-RAS International Conference on Humanoid Robots, pp. 300–305, 2011.

[2] S.H. Hyon, J. Morimoto, T. Matsubara, T. Noda, and M. Kawato, "XoR: Hybrid Drive Exoskeleton Robot That Can Balance," in Proceedings of the IEEE/RSJ Intl. Conference on Intelligent Robots and Systems, 2011

[3] T. Noda, N. Sugimoto, J. Furukawa, M. Sato, S. H. Hyon, J. Morimoto, "Brain-Controlled Exoskeleton Robot for BMI Rehabilitation, 12th IEEE-RAS International Conference on Humanoid Robots, pp. 22–27, 2012.

[4] T. Noda, J. Furukawa, T. Teramae, S.H. Hyon, and J. Morimoto, "An Electromyogram based Force Control Coordinated in Assistive Interaction," in Proceeding of the 2013 IEEE International Conference on Robotics and Automation, 2013.

[5] T. Teramae, T. Noda, S.H. Hyon and J. Morimoto, "Modeling and Control of A Pneumatic-Electric Hybrid System," in The IEEE/RSJ International Conference on Intelligent Robots and Systems, pp. 4887–4892, 2013

[6] D. H. Jacobson and D. Q. Mayne, "Differential dynamic programming, " Elsevier, 1970.

[7] E. Todorov and W. Li, "A generalized iterative LQG method for locally-optimal feedback control of constrained nonlinear stochastic systems," In Proceedings of the American Control Conference, pp. 300–306, 2005.

[8] E. Todorov, C. Hu, A. Simpkins and J. Movellan, "Identifcation and control of a pneumatic robot", 2010 3rd IEEE RAS and EMBS International Conference on Biomedical Robotics and Biomechatronics, pp. 373–380, 2010.

[9] D. Shin, I. Sardellitti, Y.-L. Park, O. Khatib, and M. Cutkosky, "Design and control of a bio-inspired human-friendly robot," International Journal of Robotics Research, vol. 29, no. 5, pp. 571–584, 2010.

[10] D. Shin, I. Sardellitti1, O. Khatib, "A Hybrid Actuation Approach for Human-Friendly Robot Design," Proceedings of the 2008 IEEE International Conference on Robotics and Automation 2008.

[11] FESTO, http://www.festo.com

[12] T. Vo-Minh, T. Tjahjowidodo, H. Ramon, H. V. Brussel, "Cascade position control of a single pneumatic artificial muscle–mass system with hysteresis compensation", Mechatronics, IEEE/ASME Transactions on, vol. 16, no. 1, pp. 177–186, 2011.

[13] C. Chou, B. Hannaford, "Measurement and modeling of McKibben pneumatic artificial muscles ", IEEE Transactions on Robotics and Automation, 12(1), pp. 90–102, 1996.

[14] K. Inoue, "Rubbertuators and applications for robots," in Proceedings of the 4th international symposium on Robotics Research. MIT Press, pp. 57–63, 1988.